

Molecular Origin of the L-Type Ca^{2+} Current of Skeletal Muscle Myotubes Selectively Deficient in Dihydropyridine Receptor β_{1a} Subunit

Caroline Strube,^{*,#} Maryline Beurg,^{*} Manana Sukhareva,^{*} Chris A. Ahern,^{*} Jeanne A. Powell,[§] Patricia A. Powers,^{||} Ronald G. Gregg,^{||} and Roberto Coronado^{*}

^{*}Department of Physiology, University of Wisconsin Medical School, Madison, Wisconsin 53706; [#]Laboratoire de Physiologie des Elements Excitables, Université Claude Bernard-Lyon 1, 69622 Villeurbanne, France; [§]Department of Biological Sciences, Smith College, Northampton, Massachusetts 01063; ^{||}Biotechnology Center, University of Wisconsin, Madison, Wisconsin 53706; and ^{||}Department of Biochemistry, University of Louisville, Louisville, KY 40202

ABSTRACT The origin of $I_{\beta\text{null}}$, the Ca^{2+} current of myotubes from mice lacking the skeletal dihydropyridine receptor (DHPR) β_{1a} subunit, was investigated. The density of $I_{\beta\text{null}}$ was similar to that of I_{dys} , the Ca^{2+} current of myotubes from dysgenic mice lacking the skeletal DHPR α_{1S} subunit (-0.6 ± 0.1 and -0.7 ± 0.1 pA/pF, respectively). However, $I_{\beta\text{null}}$ activated at significantly more positive potentials. The midpoints of the $G_{\text{Ca}}-V$ curves were 16.3 ± 1.1 mV and 11.7 ± 1.0 mV for $I_{\beta\text{null}}$ and I_{dys} , respectively. $I_{\beta\text{null}}$ activated significantly more slowly than I_{dys} . At +30 mV, the activation time constant for $I_{\beta\text{null}}$ was 26 ± 3 ms, and that for I_{dys} was 7 ± 1 ms. The unitary current of normal L-type and β_1 -null Ca^{2+} channels estimated from the mean variance relationship at +20 mV in 10 mM external Ca^{2+} was 22 ± 4 fA and 43 ± 7 fA, respectively. Both values were significantly smaller than the single-channel current estimated for dysgenic Ca^{2+} channels, which was 84 ± 9 fA under the same conditions. $I_{\beta\text{null}}$ and I_{dys} have different gating and permeation characteristics, suggesting that the bulk of the DHPR α_1 subunits underlying these currents are different. $I_{\beta\text{null}}$ is suggested to originate primarily from Ca^{2+} channels with a DHPR α_{1S} subunit. Dysgenic Ca^{2+} channels may be a minor component of this current. The expression of DHPR α_{1S} in β_1 -null myotubes and its absence in dysgenic myotubes was confirmed by immunofluorescence labeling of cells.

INTRODUCTION

The dihydropyridine receptor (DHPR) of skeletal muscle comprises α_{1S} , β_{1a} , α_2/δ , and γ subunits. This complex serves as a voltage sensor for excitation-contraction (EC) coupling and is responsible for the L-type Ca^{2+} current present in these cells. Functional expression of cDNAs in dysgenic myotubes supports the view that the α_1 subunit of the DHPR determines, to a large extent, the properties of the Ca^{2+} current and the type of EC coupling expressed in the muscle cell (Tanabe et al., 1988, 1990a,b, 1991; Adams et al., 1990; Garcia-Martinez et al., 1994; Garcia-Martinez, 1994). The dysgenic mutation consists of a single base deletion in the murine gene encoding for the α_{1S} subunit of the DHPR (Chaudhari, 1992; Varadi et al., 1995). Dysgenic myotubes do not have a functional α_{1S} subunit, yet display a low-density L-type Ca^{2+} current that has been named I_{dys} (Adams and Beam, 1989; Shimahara and Bornaud, 1991). Presumably, I_{dys} is encoded by a cardiac-type α_{1C} subunit, although this has not been entirely demonstrated (Chaudhari and Beam, 1993). I_{dys} activates much faster than, and inactivates much more slowly than, the normal L-type Ca^{2+} current (Adams and Beam, 1989). Under some conditions, I_{dys} mediates contractions that are dependent on external Ca^{2+} , suggesting that this current may play a functional role in the fetal stages of muscle development (Adams and Beam, 1991).

The function of the β subunit of the DHPR in skeletal muscle has been investigated using gene targeting to inactivate the murine gene encoding β_{1a} , the most abundant β subunit expressed in skeletal muscle (Gregg et al., 1996). Quite surprisingly, β_1 -null myotubes displayed a phenotype that is similar to that of dysgenic myotubes consisting of EC uncoupling, a low density of charge movement, and a low-density L-type Ca^{2+} current named $I_{\beta\text{null}}$ (Strube et al., 1996). Ca^{2+} currents, charge movements, and intracellular Ca^{2+} transients are restored in β_1 -null myotubes after transfection with β_{1a} cDNA (Beurg et al., 1997). These results suggest that β_1 has a critical function in modulating both the functional expression of the DHPR voltage sensor and the Ca^{2+} current.

The low density of $I_{\beta\text{null}}$, the L-type Ca^{2+} current of β_1 -null myotubes, may indicate that functional α_{1S} subunits are absent in these cells. If this is so, $I_{\beta\text{null}}$ could be similar to I_{dys} . Alternatively, $I_{\beta\text{null}}$ may represent a down-regulated L-type Ca^{2+} channel due to the specific absence of β_{1a} from the skeletal DHPR complex. In this case, $I_{\beta\text{null}}$ should differ qualitatively from I_{dys} . To clarify the molecular origin of $I_{\beta\text{null}}$, in the present study we analyzed conductive and gating properties of the L-type Ca^{2+} current of dysgenic and β_1 -null myotubes under identical conditions in primary cell cultures. Part of this work has appeared previously in abstract form (Strube et al., 1997).

MATERIALS AND METHODS

Cell cultures

Mouse myotubes homozygous for the *mdg* allele (*mdg/mdg*) or the β_1 mutation *cchbl*^{-/-} are called dysgenic and β_1 -null, respectively. Collec-

Received for publication 9 September 1997 and in final form 29 March 1998.

Address reprint requests to Dr. R. Coronado, Department of Physiology, University of Wisconsin, 1300 University Avenue, Madison, WI 53706. Tel.: 608-262-1272; Fax: 608-265-5512; E-mail: coronado@physiology.wisc.edu.

© 1998 by the Biophysical Society
0006-3495/98/07/207/11 \$2.00

tively they are called mutant cells. Mouse myotubes with a normal phenotype were heterozygous for either mutation (*mdg*⁺ or *cchb1*^{-/+}) or wild type. All experiments were performed on primary cultures as previously described (Beurg et al., 1997). The hind limbs of 18-day-old fetuses were dissected free of skin and bones and washed in Ca²⁺-Mg²⁺-free Hanks' buffer. The tissues were incubated for ~10 min at 37°C in Ca²⁺-Mg²⁺-free Hanks' buffer containing 0.125% trypsin and 0.05% pancreatin (from porcine pancreas; Sigma Chemical Co., St. Louis, MO). After mechanical dispersion, the cell suspension was filtered through sterile gauze. After centrifugation of the filtrate and resuspension of the pellet in plating medium, the cells were preplated into 100-mm Falcon plastic dishes for 1 h to enrich the myoblasts. Final plating was done in 35-mm Falcon plastic petri dishes covered with 1% gelatin at $1-4 \times 10^4$ cells/plate in 2 ml plating medium. Cells were grown in 8% CO₂ for 5–7 days and later in 5% CO₂ in fetal bovine serum-free medium. The plating medium was composed of 78% Dulbecco's modified Eagle medium, 10% horse serum, 10% fetal bovine serum, 2% chick embryo extract, 10 U/ml penicillin, and 0.01 mg/ml streptomycin. The fetal bovine serum-free medium was composed of 88.75% Dulbecco's modified Eagle medium, 10% horse serum, 1.25% chick embryo extract, 10 U/ml penicillin, and 0.01 mg/ml streptomycin.

Immunostaining

Cells were fixed and processed for immunostaining as described (Flucher et al., 1991). The DHPR α_{1S} monoclonal antibody (Upstate Biotechnology, Lake Placid, NY) was used at a dilution of 1:50. The secondary antibody was a fluorescein conjugated polyclonal goat anti-mouse IgG (Cappel, IGN Pharmaceuticals, Irvine, CA) and was used at a dilution of 1:100. Fluorescence confocal images of 512 by 512 pixels (0.1–0.3 $\mu\text{m}/\text{pixel}$) were obtained on a BioRad 1000 confocal microscope (BioRad Instruments, Hercules, CA), using the 488-nm spectral line from an argon laser. Images were converted to a 16-level gray scale with National Institutes of Health-Image software.

Ca²⁺ currents

The standard patch-clamp technique was used in the whole-cell recording configuration. Ca²⁺ current was recorded as previously described (Strube et al., 1996). The external solution for current recording was (in mM) 130 tetraethylammonium methanesulfonate, 10 CaCl₂ or 10 BaCl₂, 1 MgCl₂, 10⁻³ tetrodotoxin, and 10 HEPES-tetraethylammonium(OH), pH 7.4. The pipette solution consisted of (in mM) 140 Cs aspartate, 5 MgCl₂, 5 EGTA, 10 3-[N-morpholino]propane sulfonic acid-CsOH, pH 7.2. Standard patch electrodes had tip resistances between 2 M Ω and 5 M Ω when filled with the pipette solution. Recordings were made with an Axopatch 1D and a headstage with a 50-M Ω feedback resistor (Axon Instruments, Foster City, CA). The effective series resistance was compensated up to the point of amplifier oscillation with the analog circuit provided by Axopatch. Three linear capacitive components and a leak component were canceled with a tunable analog circuit. Data acquisition was performed with a TL1 DMA interface controlled by pCLAMP software (Axon Instruments). The data were digitized at 50–400 $\mu\text{s}/\text{point}$ and filtered at 1–3 kHz with an analog 8-pole Bessel filter. All experiments were performed at room temperature.

Variance analysis

The ensemble variance of I_{dys} and $I_{\beta\text{null}}$ was estimated from the ensemble average of the squared difference between consecutive current records (Heinemann and Conti, 1992). A set of 50 pulses to +20 mV was delivered to the same cell at a rate of one pulse every 5 s. The pulse cycle was delivered from a holding potential of -80 mV and consisted of a step to -30 mV for 750 ms, followed by the test pulse to +20 mV, followed by a step to -30 mV, followed by a step to the holding potential. Test pulse duration and sampling frequency were 25 ms and 40 kHz or 50 ms and 20 kHz for dysgenic cells. Test pulse duration and sampling frequency were 50 ms and 20 kHz or 100 ms and 10 kHz for β_1 -null and normal cells. All

records were low-pass-filtered at 4 or 2 kHz at the moment of acquisition with an 8-pole analog Bessel filter. Amplifier gain was set at 5 mV/pA, and the A/D resolution was 0.5 pA per bit. The set of 50 pulses was repeated several times, and one or two sets per cell were selected for analysis. Pairs of consecutive records $\{X_{i-1}(t), X_i(t)\}$ within a selected set were subtracted in an overlapped manner to generate 49 difference records, $\{X_i(t) - X_{i-1}(t)\}$. A maximum of 10 difference records were discarded. The ensemble variance, σ^2 (+), for the remaining records, n , was calculated according to Eq. 1 (Noceti et al., 1996):

$$\sigma^2(t) = 2/n \sum_{i=1}^n (Y(t)_i - \mu(t))^2$$

where $\mu(t)$ was the mean value of $Y(t)_i$ and $Y(t)_i = 1/2 \{X_i(t) - X_{i-1}(t)\}$. The variance at the holding potential was estimated in the same manner and was time-averaged for 10 ms before the voltage pulse. The resting variance was subtracted from $\sigma^2(t)$, and the latter plotted against the ensemble mean current, $I(t)$, of the same set of current records. The mean-variance relationship was fit by a nonlinear least-squares method according to Eq. 2 (Neher and Stevens, 1975; Sigworth, 1980),

$$\sigma^2(t) = iI(t) - I^2(t)/N_F$$

where i is the single-channel current and N_F is the number of functional channels activated by the voltage pulse. Some difference records were discarded from the analysis because of deterioration of the pipette seal resistance or excess of current run-down during the acquisition of one or both of the original current records. To discard these records objectively, i.e., without assumptions concerning the time course $\sigma^2(t)$, we ranked difference records as suggested by Heinemann and Conti (1992). We calculated the variance of the time-averaged current in three segments of each difference record, a few milliseconds before the pulse, immediately after the onset of the pulse, and immediately before the ending of the pulse. Traces with the highest numerical score in each of these time segments, up to a total of 10 traces, were discarded. In these time segments, the traces with the highest scores were the most likely to be contaminated by, respectively, an increase in resting leak, a mismatch in the cancellation of residual capacitance transients, and an increase in leak or rundown during the pulse. Variance calculations were verified using pseudomacroscopic ensemble currents generated by a single-channel simulation program (CSIM, Axon Instruments).

Data and curve fitting

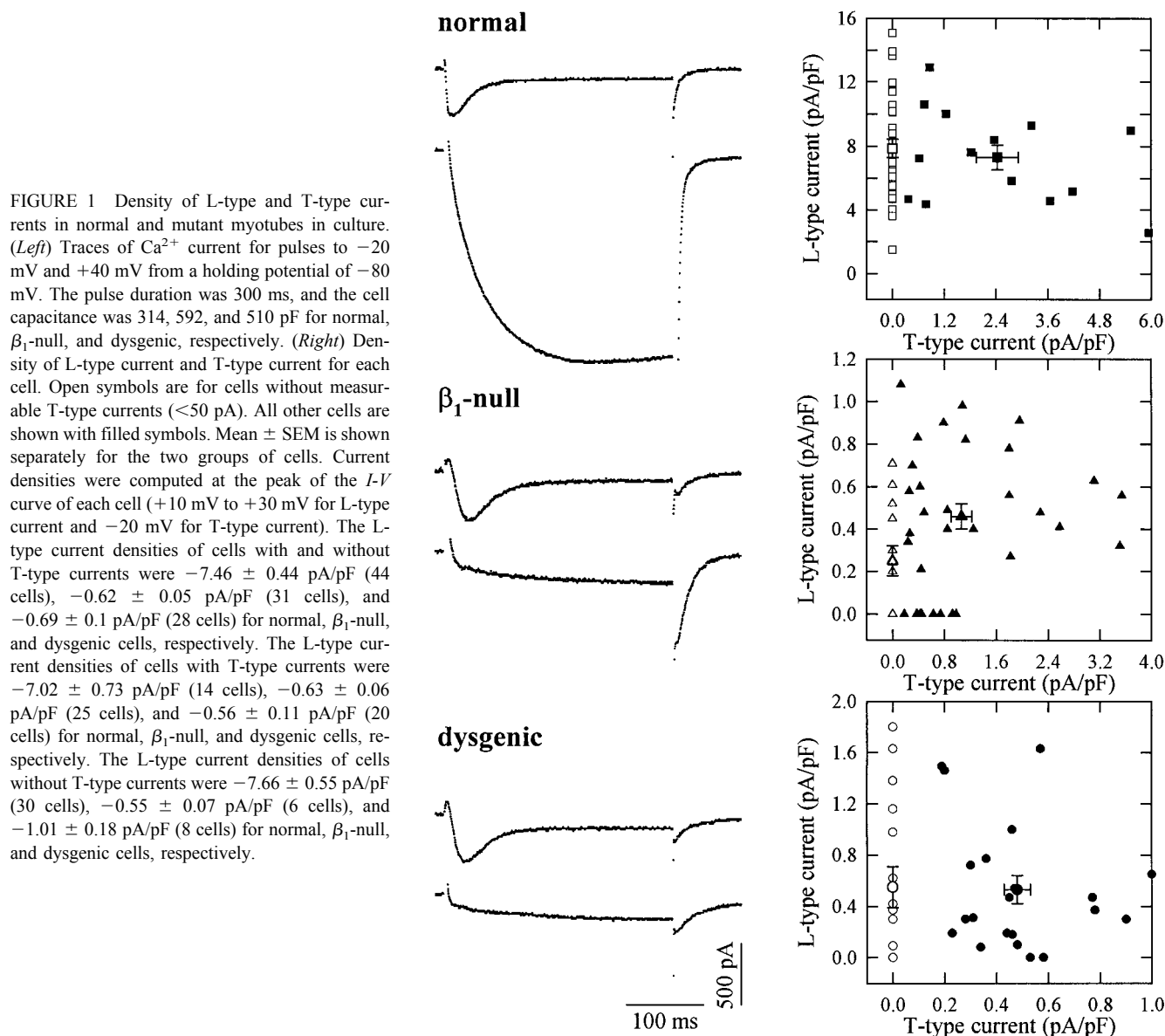
The density of the Ca²⁺ current of normal and mutant myotubes is approximately constant from days 8 to 16 of cell culture (Beurg et al., 1997). In the present study, we pooled and averaged data from cells between days 8 and 17 of culture. Curve fitting was done with Marquardt-Levenberg algorithms provided by Sigmaplot (Jandel, San Rafael, CA) and pClamp (Axon Instruments). The time constant τ_1 , describing activation of the Ca²⁺ current, was obtained from a fit of the pulse current at each voltage according to $I(t) = K[1 - \exp(-t/\tau_1)]\exp(-t/\tau_2)$ (Eq. 3), where K is a constant and τ_2 describes inactivation. All averages are presented as mean \pm SEM.

Chemicals

Deionized glass-distilled water was used in all solutions. All salts were reagent grade. Bay K 8644 was made as 5 mM stocks in absolute ethanol and stored in light-resistant containers. TTX was from Sigma Chemical Co. Bay K 8644 was from Calbiochem (La Jolla, CA).

RESULTS

Fig. 1 shows Ca²⁺ currents in normal, β_1 -null, and dysgenic cells in culture. The transient component was in response to



a pulse to -20 mV from a holding of -80 mV and was identified as T-type current (Adams and Beam, 1989; Strube et al., 1996). The sustained component shown in the bottom trace was in response to a pulse to $+40$ mV and was identified as L-type current in all cases. The sustained currents of the two mutant cells, here identified as $I_{\beta_{\text{null}}}$ and I_{dys} , were much smaller than the L-type current of normal cells. This result is in agreement with previous studies performed separately in dysgenic and β_1 -null myotubes in culture (Bournaud et al., 1989; Beurg et al., 1997). L-type and T-type components were not always present in each cell. This is shown in the right panels of Fig. 1, in which the density of L-type current is plotted in the abscissa, and the density of T-type current in the same cell is plotted in the ordinate. The open symbols correspond to cells without a detectable T-type current, whereas the filled symbols cor-

respond to cells in which T-type currents were obvious. The population average density of the L-type current was computed separately for cells with or without T-type currents and is indicated in each graph. The presence or absence of T-type currents did not influence the L-type Ca²⁺ current density, except in the case of β_1 -null cells, where the L-type current was lower in the subpopulation of cells without T-type current. This correlation was weak, and it did not extend to other properties of the L-type current of β_1 -null cells, such as the kinetics of activation and sensitivity to Bay K 8644 described below. L-type Ca²⁺ currents were present in all normal cells (61 cells), about two-thirds of β_1 -null cells (48 of 67 cells), and about two-thirds of dysgenic cells (52 of 67 cells). L-type and T-type Ca²⁺ currents were present in about one-third of all normal cells and about five-sixths of all mutant cells. In the remainder of this study,

recordings were made either from a holding potential of -50 or -40 mV to inactivate the T-type current, or from -80 mV in cells without T-type currents.

Fig. 2 shows L-type Ca^{2+} currents in response to 1-s pulses from a holding potential of -50 mV in a normal, a β_1 -null, and a dysgenic myotube. Currents were normalized to the cell capacitance, and it should be noticed that scales for normal and mutant cells are different. At all pulse potentials, the normal Ca^{2+} current was much larger than either $I_{\beta\text{null}}$ or I_{dys} . In addition, the normal current had a slower time to peak and displayed significant inactivation. The mutant currents had a similar density and showed little inactivation during the pulse. Current-voltage relationships are shown in the top panel of Fig. 3. The three Ca^{2+} currents activated at potentials more positive than -10 mV, but the peak densities of $I_{\beta\text{null}}$ and I_{dys} were 11- to 12-fold lower than the peak density of the normal current. Furthermore, I_{dys} activated at slightly more negative potentials than $I_{\beta\text{null}}$. The bottom panel of Fig. 3 shows conductance-voltage relationships for the two mutant currents. A Boltzmann fit of the $G_{\text{Ca}}-V$ curve of 31 β_1 -null cells and 25 dysgenic cells showed that G_{max} (30.2 ± 2.5 pS/pF for β_1 -null versus 30.5 ± 3.5 pS/pF for dysgenic) and the slope factor k (8.6 ± 0.4 mV versus 8.7 ± 0.4 mV) were identical for the two currents. However, there was a ~ 5 mV difference in $V_{1/2}$ (16.3 ± 1.1 mV versus 11.7 ± 1.0 mV) that was significant ($p < 0.005$, unpaired t -test). This result suggested that the voltage dependences of the DHPR complexes underlying $I_{\beta\text{null}}$ and I_{dys} were nonidentical.

To more fully understand the molecular nature of the DHPR complexes underlying $I_{\beta\text{null}}$ and I_{dys} , we investigated permeation, activation kinetics, and pharmacological properties of both currents. Fig. 4 shows current-voltage curves of β_1 -null and dysgenic cells in which the external solution

containing 10 mM Ca^{2+} was replaced by 10 mM Ba^{2+} and then returned to 10 mM Ca^{2+} . In some experiments, this sequence was reversed so that Ba^{2+} was replaced with Ca^{2+} , and then the external solution was returned to Ba^{2+} . In all cases, the Ba^{2+} current was larger than the Ca^{2+} current by an average proportion of ~ 1.7 -fold for $I_{\beta\text{null}}$ and ~ 1.9 -fold for I_{dys} . This result was consistent with the identification of $I_{\beta\text{null}}$ and I_{dys} as L-type currents. However, there was a much larger separation of the $I_{\text{Ba}}-V$ and $I_{\text{Ca}}-V$ curves in β_1 -null cells than in dysgenic cells. This is clearly seen in the normalized curves shown in the bottom panels of Fig. 4. The asterisks indicate Ca^{2+} and Ba^{2+} currents that at the same potential were significantly different ($p < 0.02$, unpaired t -test). Evidently, Ca^{2+} biased the voltage dependence of $I_{\beta\text{null}}$ more strongly than that of I_{dys} .

Fig. 5 shows scaled traces of the time course of normal, $I_{\beta\text{null}}$, and I_{dys} currents for a depolarization to $+20$ mV. I_{dys} activated faster than $I_{\beta\text{null}}$, and both activated faster than the normal current. Furthermore, $I_{\beta\text{null}}$ and I_{dys} displayed much less inactivation than the normal current. In fact, the inactivation of I_{dys} or $I_{\beta\text{null}}$ was barely detectable in most cases. The lines correspond to a fit of the pulse current according to Eq. 3. In most cells, this equation was sufficient to describe the time course of the Ca^{2+} current in the range of positive potentials. From the fit we extracted the time constant of current activation, which is shown at each voltage and for each cell type in the bottom panel of Fig. 5. I_{dys} activated two- to threefold faster than $I_{\beta\text{null}}$ and fivefold faster than the normal current. Furthermore, in this range of test potentials the activation rate of I_{dys} was essentially voltage-independent. In contrast, the activation rate of the normal and $I_{\beta\text{null}}$ currents slowed with increasingly positive potentials. The slowing of the normal current at positive

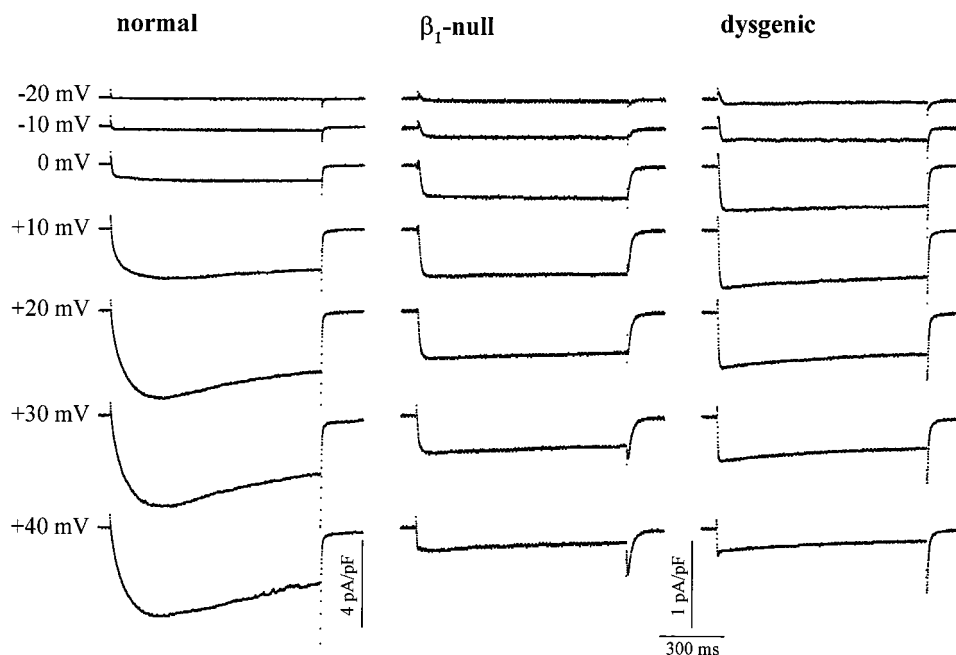


FIGURE 2 Voltage dependence of normal and mutant Ca^{2+} currents. Whole-cell L-type Ca^{2+} currents are shown for a normal, β_1 -null, and dysgenic myotube at the indicated pulse potentials. The holding potential was -50 mV, and the pulse duration was 1 s. The cell capacitance was 267, 522, and 718 pF for the normal, β_1 -null, and dysgenic cells, respectively.

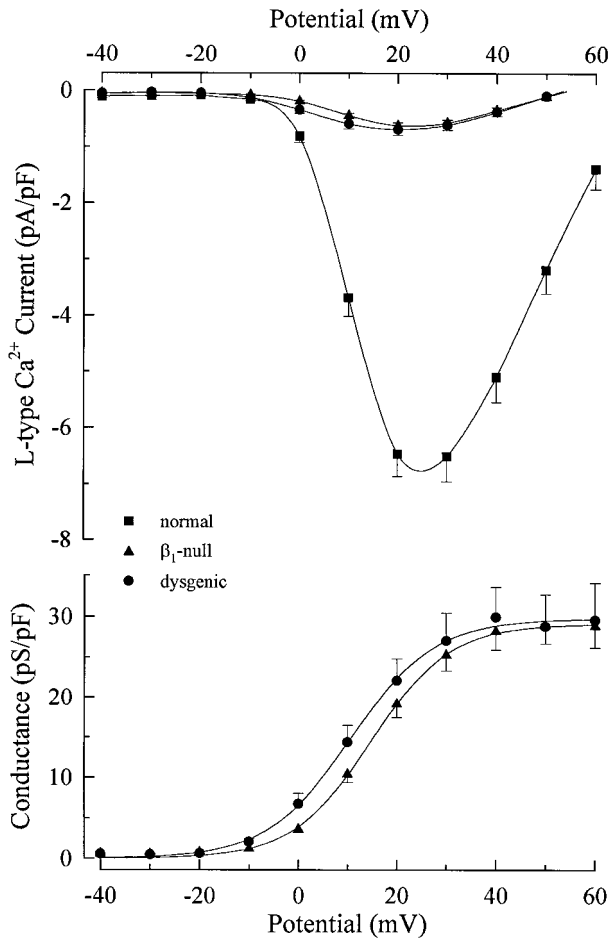


FIGURE 3 Current-voltage and conductance-voltage relationships of normal and mutant Ca²⁺ currents. (Top) Voltage dependence of the L-type Ca²⁺ current measured 300 ms after the onset of the pulse in normal (■, 45 cells), β_1 -null (▲, 31 cells), and dysgenic (●, 28 cells) myotubes. (Bottom) Voltage dependence of the L-type Ca²⁺ conductance of β_1 -null (▲, 31 cells) and dysgenic (●, 25 cells) myotubes. The lines are a Boltzmann fit to the population average G_{Ca} - V curves. Parameters of the fit are $G_{max} = 29.2$ and 29.8 pS/pF; $V_{1/2} = 14.8$ and 10.7 mV; $k = 7.9$ and 8.4 mV for β_1 -null and dysgenic myotubes, respectively.

potentials was similar to that described previously (Dirksen and Beam, 1995).

The stimulatory effects of the DHP Bay K 8644 are shown in Fig. 6. When cells were exposed to $5 \mu\text{M}$ Bay K 8644, the peak Ca²⁺ current increased by ~ 1.3 -fold in normal, ~ 2.1 -fold in β_1 -null, and ~ 2.7 -fold in dysgenic myotubes. Thus I_{dys} was stimulated more strongly than $I_{\beta null}$. However, the difference was not significant (t -test, $p = 0.2$). Because Bay K 8644 is known to reduce the time to peak of the L-type current, we also investigated whether the kinetics of activation of each current were affected differently. The bottom panel of Fig. 6 shows time constants of activation fitted to the pulse current in the range of -10 to $+40$ mV in cells stimulated by $5 \mu\text{M}$ Bay K 8644. A comparison of time constants in Figs. 5 and 6 indicated that the DHP accelerated the kinetics of activation in all cases. However, the activation time constant was reduced more

strongly in normal and β_1 -null cells than in dysgenic cells. The ranking order for stimulation of the Ca²⁺ current was $I_{dys} > I_{\beta null} > \text{normal}$, whereas that for stimulation of the activation rate was $\text{normal} > I_{\beta null} > I_{dys}$. This result suggested that the DHPR complexes responsible for $I_{\beta null}$ and I_{dys} displayed different mechanisms of modulation by DHPs.

Fig. 3 showed that the densities of $I_{\beta null}$ and I_{dys} were the same. However, the properties of the Ca²⁺ channels underlying these currents, namely, the unitary single-channel current, i , and the number of functional channels per cell, N_F , may not necessarily be identical. Thus we estimated i and N_F by mean-variance analysis. Fig. 7, A–C, shows the time course of the mean Ca²⁺ current (*smooth trace*) and its variance (*noisy trace*) estimated from 40 pulses to $+20$ mV in a normal, a β_1 -null, and a dysgenic cell. In the normal cell, the variance increased in proportion to the mean current throughout the pulse. In contrast, the variance of $I_{\beta null}$ and I_{dys} saturated earlier than the mean current. To increase the accuracy of the variance determination, we selected mutant cells with relatively large current densities. I_{max} , the whole-cell Ca²⁺ current measured at the end of the pulse, was 0.5 – 2 pA/pF for the mutant cells and 4 – 7 pA/pF for normal cells. In cells with $I_{max} < 0.2$ pA/pF, the variance of the pulse current was barely distinguishable from the variance of the rest current immediately before the pulse. The latter component was subtracted from the pulse variance in all cases. After normalization for cell capacitance, the variance of $I_{\beta null}$ at times longer than the activation time constant amounted to a doubling of the rest variance, whereas those of I_{dys} or the normal current were at least three times as large. Hence I_{dys} was intrinsically noisier than $I_{\beta null}$. This is clearly noticeable in a comparison of variance traces in Fig. 7, B and C, during the second half of the pulse. Fig. 7, D–F, shows mean-variance curves of the same data. The smooth line is a fit of the data according to Eq. 2. In agreement with the shape of each curve, N_F was the largest and p_{max} (I_{max}/iN_F) the lowest for normal cells. Because of the uncertainty in the fit of a quasilinear mean-variance curve with Eq. 2, for normal cells we could only estimate N_F as >300 channels/pF and $p_{max} < 0.3$ (six cells). In mutant cells, the mean-variance curves reached a maximum in all cases, and the parabolic fit resulted in unique parameters. For five β_1 -null cells N_F was 45 ± 12 channels/pF and p_{max} was 0.68 ± 0.1 , and for five dysgenic cells N_F was 24 ± 5 channels/pF and p_{max} was 0.62 ± 0.1 . Evidently, a similar p_{max} was reached at the end of the pulse by the Ca²⁺ channels of β_1 -null and dysgenic cells. Furthermore, I_{max} for these two groups of cells was the same (1 ± 0.2 pA/pF versus 1.4 ± 0.5 pA/pF, respectively), and the difference in channel density was not significant (t -test, $p = 0.13$). The initial slope of the mean-variance curve was much larger for dysgenic cells than for the other two cell types and resulted in a fitted i that was larger for the dysgenic cells. This is best shown by plots of the ratio variance/mean versus mean (Fig. 7, G–I). Because Eq. 2 can be rearranged as $\sigma^2(t)/I(t) = i -$

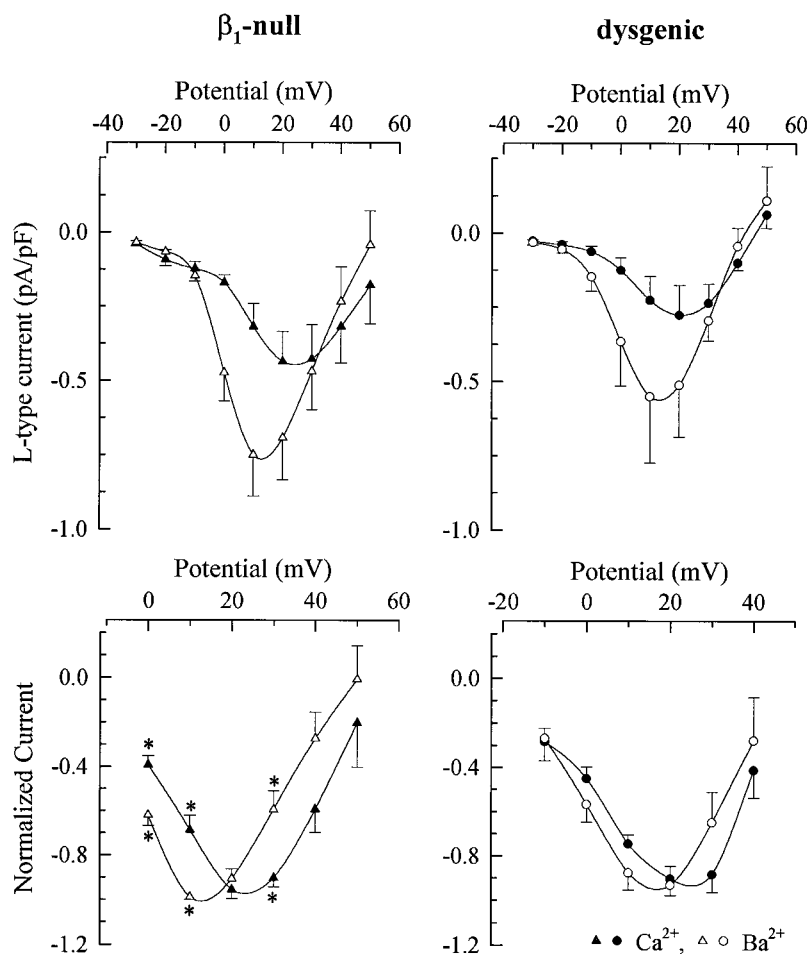


FIGURE 4 Ca^{2+} and Ba^{2+} current-voltage relationships for $I_{\beta_{\text{null}}}$ and I_{dys} . (Top left and right) L-type $I-V$ curves for the same β_1 -null (five cells) or dysgenic (five cells) cells in external solution containing 10 mM Ca^{2+} (filled symbols) and 10 mM Ba^{2+} (open symbols). (Bottom left and right) The same data normalized to the peak of the $I-V$ curve. The asterisks indicate Ca^{2+} and Ba^{2+} currents that were significantly different at the same potential (unpaired t -test, $p < 0.02$).

$(1/N_F)I(t)$, the single-channel current i may be conveniently obtained by linear extrapolation of the variance/mean ratio to zero mean current. The data showed that the extrapolated y intercept (i) was higher for I_{dys} than for either $I_{\beta_{\text{null}}}$ or the normal current. The single-channel currents obtained by extrapolation of the ratio-mean plot and those obtained from the parabolic fit of the mean-variance plot were in close agreement and were (in fA) 22 ± 4 (six cells), 43 ± 7 (five cells), and 84 ± 9 (five cells) for normal, β_1 -null, and dysgenic cells. In all combinations, these differences were significant (t -test, $p < 0.02$). It should be noted that the accuracy of the fit of N_F is low unless the mean-variance relationship is highly curved. This was not the case for all cells. On the other hand, i is fit with the same accuracy in mean-variance plots with high or low curvature, as long as the time course of the variance at low $I(t)$ is accurate. In summary, the mean-variance analysis demonstrated that the Ca^{2+} permeation characteristics of dysgenic and β_1 -null Ca^{2+} channels were significantly different.

Many properties of $I_{\beta_{\text{null}}}$ shown here and previously are consistent with the bulk of this current originating from a DHPR complex that includes the α_{1S} subunit (Strube et al., 1996; Beurg et al., 1997). However, conventional epifluorescence of β_1 -null cells labeled with a α_{1S} monoclonal

antibody failed to detect significant levels of expression of α_{1S} (Gregg et al., 1996). We reexamined this question by immunolabeling cells at a higher antibody concentration (1:50 dilution instead of 1:200 used previously) and with a different α_{1S} monoclonal antibody (Ohlendieck et al., 1991). Fig. 8 shows confocal gray scale images of a dysgenic (A) and β_1 -null (B) myotubes labeled with a α_{1S} -specific primary antibody and a fluorescein-conjugated secondary antibody. We consistently observed a faint staining of the dysgenic myotubes. The latter result agreed with a previous report (Flucher et al., 1991) and presumably was due to nonspecific secondary antibody binding to the myotube. Background-level staining of cells of the kind observed in Fig. 8 A was also seen in many β_1 -null cells (not shown). However, $\sim 50\%$ of the examined β_1 -null myotubes displayed a fluorescence intensity significantly above the background intensity. The image in Fig. 8 B was representative of β_1 -null myotubes displaying a high immunofluorescence. Evidently, α_{1S} was expressed in some but not all β_1 -null myotubes in culture. The fact that $\sim 50\%$ of β_1 -null cells did not express α_{1S} was consistent with the finding that $\sim 30\%$ of the β_1 -null myotubes did not display L-type Ca^{2+} current, although no efforts were made to explore this correlation further.

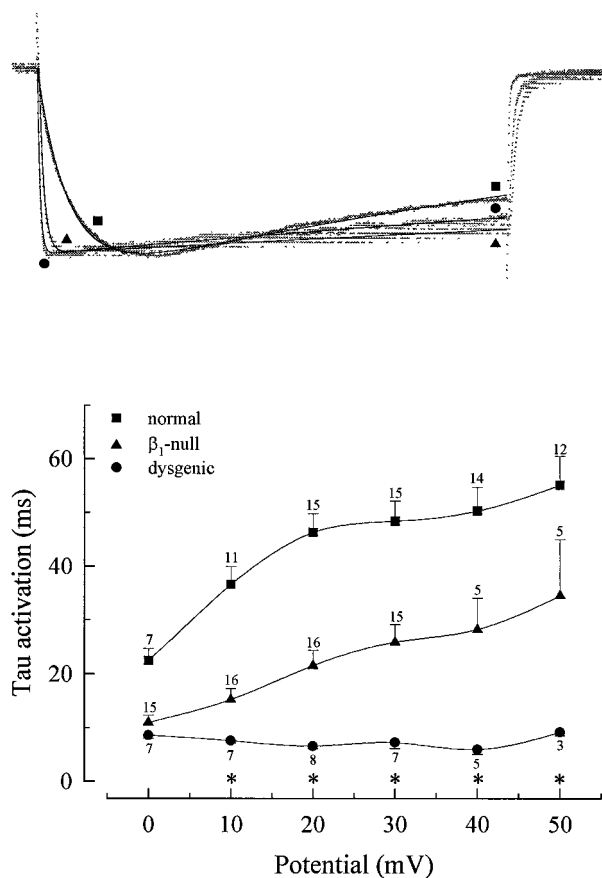


FIGURE 5 Kinetics of activation of $I_{\beta\text{null}}$ and I_{dys} . (Top) Scaled traces at +20 mV of normal L-type Ca²⁺ current (■), $I_{\beta\text{null}}$ (▲), and I_{dys} (●) in response to a 1-s pulse from a holding potential of -50 mV. The solid lines correspond to a fit of the pulse current according to Eq. 3, with $K = -1.16$ pA, $\tau_1 = 68.6$ ms, $\tau_2 = 1824$ ms for normal, $K = -1.00$ pA, $\tau_1 = 16.3$ ms, $\tau_2 = 6349$ ms for β_1 -null, and $K = -1.00$ pA, $\tau_1 = 7.6$ ms, $\tau_2 = 4251$ ms for dysgenic myotubes. (Bottom) Tau activation, τ_1 of Eq. 3, obtained from a fit of the pulse current at each potential. Entries indicate the number of cells. Asterisks indicate τ_1 for $I_{\beta\text{null}}$ and I_{dys} significantly different at the same potential (unpaired *t*-test, $p < 0.005$).

DISCUSSION

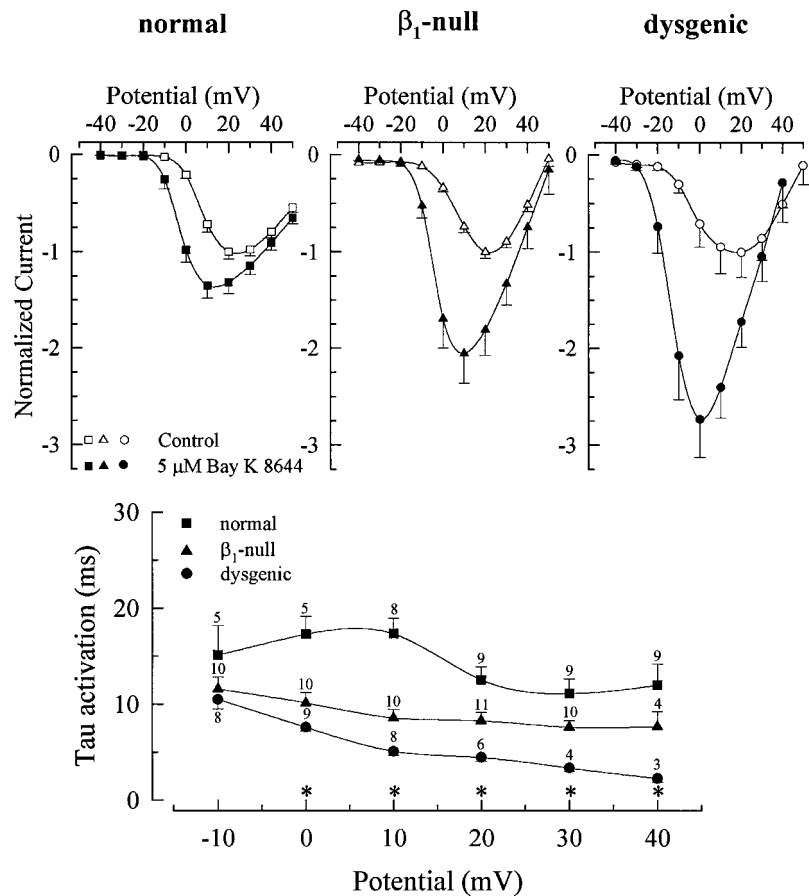
β_1 -null myotubes display an L-type Ca²⁺ current that differs from the normal L-type Ca²⁺ current in density, voltage dependence, and kinetics of activation (Strube et al., 1996; Beurg et al., 1997). $I_{\beta\text{null}}$ has many characteristics of the Ca²⁺ current produced by DHPR α_1 subunits expressed in the absence of DHPR β subunits (summarized by Strube et al., 1996). Thus $I_{\beta\text{null}}$ could originate from skeletal-type DHPR complexes that include α_{1S} but are deficient in β_{1a} . To address this issue, we compared $I_{\beta\text{null}}$ with I_{dys} , the L-type Ca²⁺ current of dysgenic myotubes that do not express a functional DHPR α_{1S} (Knudson et al., 1989; Chaudhari, 1992; Varadi et al., 1995). Statistically significant differences were found in the midpoint of the *G-V* curves, the kinetics of activation, and the single-channel currents estimated by ensemble variance analysis.

Because i estimated for $I_{\beta\text{null}}$ is between the values estimated for the normal current and for I_{dys} , $I_{\beta\text{null}}$ could

represent a mixed population of L-type channels. Some channels in this mixture could include the DHPR α_{1S} subunit, whereas others include the α_1 -dysgenic subunit. We based this explanation on the fact that a significant fraction of β_1 -null cells expressed DHPR α_{1S} and that there is no reason to assume that α_1 -dysgenic may not be expressed in these cells as well. To test this hypothesis, we performed mean-variance analysis of ensemble currents generated by computer simulation of two independent channels of different single-channel currents. The estimated i varied in direct proportion to the number of trials of each channel included in the ensemble (not shown). Assuming that i estimated for β_1 -null represents a weighted sum of the single-channel currents of x dysgenic channels and $(1 - x)$ α_{1S} channels, then $i_{\beta\text{null}} = i_{\text{dys}}x + i_{\alpha_{1S}}(1 - x)$ and $x \approx 0.34$. According to this two-channel population model for $I_{\beta\text{null}}$, the fraction of dysgenic and α_{1S} channels in β_1 -null cells would be roughly one-third and two-thirds, respectively. Thus the bulk of the Ca²⁺ channels of $I_{\beta\text{null}}$ would have α_{1S} as their pore subunit. We also considered two alternative explanations, that $I_{\beta\text{null}}$ was produced by a novel DHPR α_1 subunit with a distinct unitary conductance, and that a single type of DHPR complex without β was responsible for the estimated single-channel current of β_1 -null cells. Both explanations were considered unlikely. First, splice variants of α_{1S} that could account for this putative subunit have not been reported. Second, mutagenesis experiments have shown that the single-channel conductance of Ca²⁺ channels is determined by domains of the α_1 subunit (Yang et al., 1993; Dirksen et al., 1997) and is the same when α_1 is expressed alone or coexpressed with β subunits (Bourinet et al., 1996).

The maximum open channel probability, p_{max} , estimated by variance analysis in dysgenic, β_1 -null, and some normal cells was significantly higher than previously determined by cell-attached patch recordings. In normal myotubes, p_{max} measured in many-channel patches in the presence of Bay K 8644 was 0.19 (Dirksen and Beam, 1995). In the absence of Bay K 8644, as in our case, this value is expected to be even lower. On the other hand, p_{max} is ~ 0.3 in cardiac L-type Ca²⁺ channels. Similar values were estimated by single-channel recordings and by whole-cell variance analysis in the absence of Bay K 8644 (Tsien et al., 1986). It is entirely possible that a few Ca²⁺ channels in normal, dysgenic, and β_1 -null cells may have a high p_{max} , but the majority of them would have a low p_{max} and contribute little to the mean Ca²⁺ current or variance. Furthermore, dysgenic channels are intrinsically noisier than normal channels, and if their p_{max} is similar to that of cardiac channels, they could increase the p_{max} estimated in the β_1 -null cell. In any case, the discrepancy in p_{max} does not compromise the estimation of single-channel currents. When we separated normal cells with high and low p_{max} , the single-channel currents estimated in the two groups were similar (not shown). Finally, the mean-variance data were consistent with the noise spectra of $I_{\beta\text{null}}$ and I_{dys} when measured near steady-state (not shown). The limiting noise power at low frequencies, $S(0)$, and the cutoff frequency, $f_{1/2}$, were lower for $I_{\beta\text{null}}$ than for

FIGURE 6 Stimulation of $I_{\beta\text{null}}$ and I_{dys} by Bay K 8644. (Top) L-type I - V curves of normal, β_1 -null, and dysgenic myotubes during a control period (open symbols) and 10 min after exposure of cells to 5 mM Bay K 8644 (filled symbols). Current was normalized to the peak of the I - V curve during the control period. The fold stimulation of the peak Ca^{2+} current produced by Bay K 8644 was 1.3 ± 0.1 (11 cells) for normal, 2.1 ± 0.3 (11 cells) for β_1 -null, and 2.7 ± 0.3 (11 cells) for dysgenic myotubes. (Bottom) Activation time constants of the normal L-type current (squares), $I_{\beta\text{null}}$ (triangles), and I_{dys} (circles) in myotubes exposed to 5 μM Bay K 8644. The pulse current at each potential was fitted by Eq. 3. Tau activation corresponds to τ_1 of Eq. 3. Entries indicate the number of cells. Asterisks indicate τ_1 for $I_{\beta\text{null}}$ and I_{dys} significantly different at the same potential (unpaired t -test, $p < 0.005$). Tau activation at +30 mV in the absence and presence of Bay K 8644 was 49.2 ± 2.6 and 11.2 ± 1.5 ms (9 cells) for normal, 26 ± 3.3 and 7.6 ± 0.7 ms (10 cells) for β_1 -null, and 7.3 ± 1.1 and 3.4 ± 0.3 ms (4 cells) for dysgenic myotubes. The fold decrease in tau activation at +30 mV produced by Bay K 8644 was 4.4 ± 0.2 for normal, 3.4 ± 0.4 for β_1 -null, and 2.1 ± 0.3 for dysgenic myotubes.



I_{dys} . Both results were expected, because $S(0)$ increases with the square of the single-channel current and I_{dys} is a faster current (Conti et al., 1975).

To identify the subunit composition of $I_{\beta\text{null}}$, we first considered that of I_{dys} . The latter Ca^{2+} current could conceivably originate from DHPR complexes that include α_{1C} . Chaudhari and Beam (1993) showed that mRNA for the cardiac α_{1C} subunit is abundant in dysgenic and normal muscle. Furthermore, mRNA for α_{1C} has been reported in a dysgenic cell line (Varadi et al., 1995), as well as in primary cultures of normal myotubes (Bulteau et al., 1977) and in normal adult rodent skeletal muscle (Pereon et al., 1997). Cardiac-type Ca^{2+} currents are also present in the dysgenic cell line (Varadi et al., 1995). On the other hand, there appears to be a kinetic mismatch between the appearance of cardiac mRNA, which is higher in young fetal myotubes and declines thereafter (Chaudhari and Beam, 1993), and the appearance of I_{dys} , which has roughly the same density throughout fetal development (Shimahara and Bornaoud, 1991). Because targeting of α_1 subunits to the transverse tubules may require other DHPR subunits (Flucher et al., 1991; Chien et al., 1995), the appearance of the Ca^{2+} current may be controlled by the expression levels of α_1 as well as by other factors. Additional support for a cardiac origin of I_{dys} comes from its functional profile, which is entirely consistent with that of a cardiac L-type Ca^{2+} current. In agreement with Adams and Beam (1989), our data

showed that I_{dys} activated much faster and was stimulated more strongly by Bay K 8644 than the normal L-type current. Although I_{dys} did not inactivate during prolonged depolarization, it should be noticed that α_{1C} does not either when expressed in dysgenic myotubes (Tanabe et al., 1990b; Adams et al., 1990). Finally, the mean-variance analysis provides a compelling reason to suspect that I_{dys} is a cardiac-type current. The estimated single-channel current of ~ 84 fA in 10 mM Ca^{2+} at +20 mV is consistent with estimations made by the same technique in ventricular myocytes, which were 130 fA in 10 mM external Ba^{2+} at +10 mV (Bean et al., 1984). In summary, our results are entirely consistent with I_{dys} originating from DHPR complexes that include α_{1C} or an unidentified embryonic homolog of α_{1C} .

Based on the conclusion above, we considered the possibility that I_{dys} and $I_{\beta\text{null}}$ originated from DHPR complexes of the same " α_{1C} "-like subunit, but that complexes underlying $I_{\beta\text{null}}$ lacked β_{1a} , the isoform found in skeletal muscle and absent in the β_1 -null myotube. In heterologous systems, β_{1a} produces a negative shift of the I - V curve of α_{1C} Ca^{2+} channels, decreases the sensitivity of the Ca^{2+} current to Bay K 8644, and increases the Ca^{2+} current density (Singer et al., 1991; Wei et al., 1991; Lory et al., 1993; Nishimura et al., 1993; Perez-Garcia et al., 1995; Kamp et al., 1996). The effect of β_{1a} on the kinetics of activation of α_{1C} Ca^{2+} channels is more complex. Some investigators found an

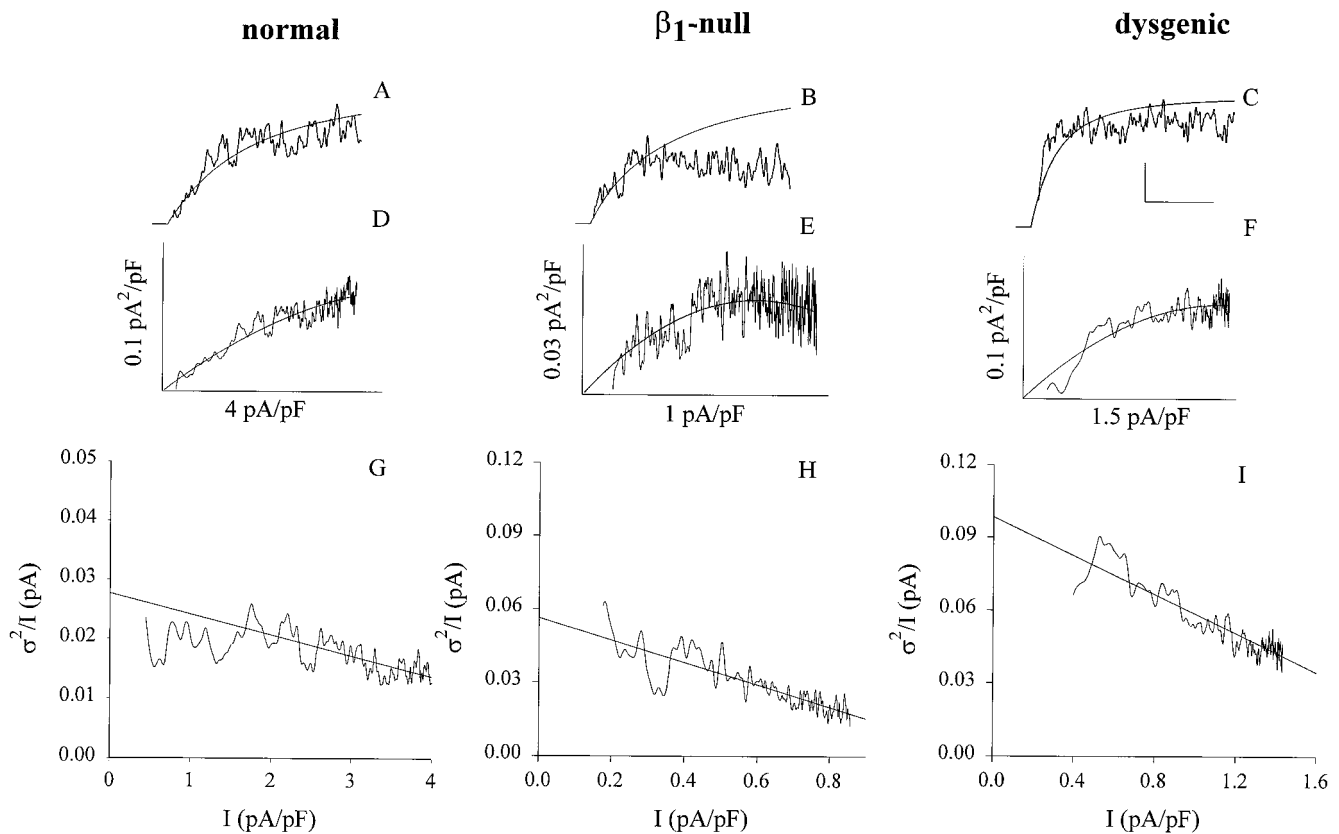


FIGURE 7 Mean-variance relationship of the normal L-type Ca²⁺ current, $I_{\beta\text{null}}$ and I_{dys} . (A–C) Superimposed time courses of the mean whole-cell Ca²⁺ current (smooth trace) and the ensemble variance (noisy trace) for a step potential to +20 mV after a 750-ms prepulse to –35 mV from a holding potential of –80 mV. The pulse duration was 100 ms for the normal cell and 50 ms for the β_1 -null and dysgenic cells. The ensemble variance was computed according to Eq. 1 from 40 pulses (39 difference traces). Variance traces were low-pass filtered at 1 kHz with a digital Gaussian filter. The vertical calibration bar corresponds to $I = 1$ pA/pF and $\sigma^2 = 0.02$ pA²/pF for normal, $I = 0.2$ pA/pF and $\sigma^2 = 0.005$ pA²/pF for β_1 -null, and $I = 0.4$ pA/pF and $\sigma^2 = 0.02$ pA²/pF for dysgenic cells. The horizontal calibration bar corresponds to 20 ms for normal and 10 ms for β_1 -null and dysgenic cells. (D–F) The ensemble variance plotted as a function of the mean Ca²⁺ current for the same cells. The origin of each graph is given by the intersection of the horizontal calibration bar (mean) and vertical calibration bar (variance). Lines are a fit of the data according to Eq. 1. Parameters of the fit are i (pA) = 0.02, 0.05, 0.08 and N_F (channels/pF) = 575, 24, 39 for normal, β_1 -null, and dysgenic, respectively. (G–I) A linear fit of the variance/mean ratio plotted as a function of the mean current.

increase in the activation rate (Singer et al., 1991; Wei et al., 1991; Lory et al., 1993); others showed no effect (Itagaki et al., 1992) or even a decrease in the activation rate (Perez-Garcia et al., 1995), none of which seemed to correlate with the expression system. We reasoned that if $I_{\beta\text{null}}$ originated

from the same DHPR complex as I_{dys} but without β_{1a} , differences between $I_{\beta\text{null}}$ and I_{dys} would be analogous to those observed when α_{1C} is expressed alone or α_{1C} is coexpressed with β_{1a} , respectively. The activation of I_{dys} at more negative potentials than $I_{\beta\text{null}}$ (Fig. 3) and the faster

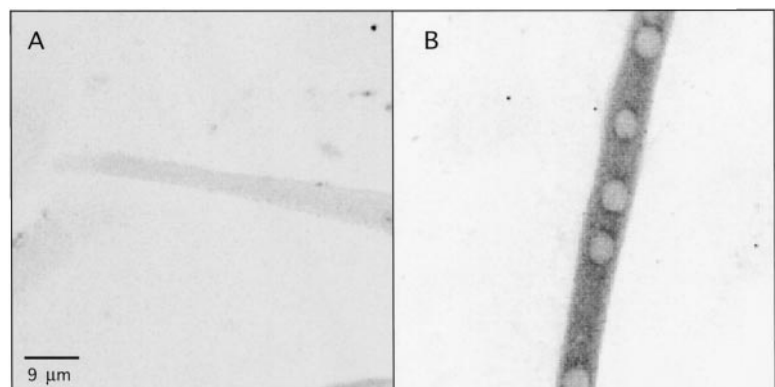


FIGURE 8 Immunofluorescence of β_1 -null and dysgenic myotubes labeled with DHPR α_{1S} antibody. Confocal images of 512×512 pixels were converted to a 16-level gray scale, and the color table was inverted so that high-intensity pixels appear black and low-intensity pixels appear white. (A) A dysgenic myotube. (B) A β_1 -null myotube at the same magnification.

activation rate of I_{dys} (Figs. 5 and 6) fit this scenario. With respect to the first observation (Fig. 3), it must be pointed out that not only β subunits but also α_1 subunits produce strong effects on the midpoint of the G - V relationship. In dysgenic myotubes the G - V curve of expressed α_{1C} Ca^{2+} channels is ~ 20 mV more negative than that of expressed α_{1S} Ca^{2+} channels (Garcia-Martinez et al., 1994). Hence the fact that I_{dys} activates at more negative potentials than $I_{\beta\text{null}}$ may not be explained solely by the presence of β_{1a} in the Ca^{2+} channel complex of I_{dys} and its absence from the $I_{\beta\text{null}}$ complex. Against the hypothesis that I_{dys} and $I_{\beta\text{null}}$ differ by the presence or absence of the β_{1a} subunit, respectively, is the observation that Bay K 8644 stimulated I_{dys} more strongly than $I_{\beta\text{null}}$. In heterologous expression systems, Ca^{2+} currents from α_{1S} and β_{1a} subunits or α_{1C} and β_{1a} subunits are always less sensitive to the agonist than those from β -deficient complexes (Varadi et al., 1991; Singer et al., 1991; Lory et al., 1992; Itagaki et al., 1992; Hullin et al., 1992). A similar observation has been made in the β_1 -null myotube, where expression of β_{1a} results in a reduction in the sensitivity of the rescued Ca^{2+} current to Bay K 8644 (Beurg et al., 1997). Exemptions to this rule are found in the expression of $\alpha_{1C}\beta_{2a}$ (Perez-Reyes et al., 1992; but see Hullin et al., 1992, for a different result), $\alpha_{1C}\beta_4$, and $\alpha_{1S}\beta_4$ (Castellano et al., 1993). In these cases, the sensitivity of the Ca^{2+} current to Bay K 8644 was unchanged by coexpression of α_1 and β subunits. Clearly, however, none of these cases involved β_{1a} . In summary, the higher sensitivity of I_{dys} to Bay K 8644 and the fact that $I_{\beta\text{null}}$ and I_{dys} had the same current density are not in keeping with the hypothesis that I_{dys} and $I_{\beta\text{null}}$ differ only by the presence or absence of DHPR β_{1a} .

The immunodetection of DHPR α_{1S} in β_1 -null and its absence in dysgenic myotubes agreed with the hypothesis that α_{1S} is a component of $I_{\beta\text{null}}$. DHPR α_{1S} was previously thought to be present at extremely low levels in β_1 -null myotubes (Gregg et al., 1996). In the present study we used a different and, evidently, a higher-affinity antibody to show significant expression of this subunit in β_1 -null myotubes in culture. The distribution of DHPR α_{1S} in β_1 -null cells differed from that reported in normal cells in several respects. Unlike in normal myotubes, a significant fraction of β_1 -null myotubes did not express DHPR α_{1S} . This observation agreed with the fact that $\sim 30\%$ of β_1 -null myotubes had undetectable levels of L-type Ca^{2+} current. Furthermore, the α_{1S} immunolabeling of β_1 -null myotubes lacked the punctuate appearance seen in normal cells (Gregg et al., 1996) and was dimmer than the immunofluorescence of normal myotubes, although well above background levels. The nonclustered distribution of α_{1S} in β_1 -null cells is consistent with the low density of tetrads observed in freeze fractures (Protasi and Franzini-Armstrong, unpublished observations) and suggests that α_{1S} is not found in triadic junctions. In this respect, the distribution of DHPR α_{1S} in β_1 -null myotubes may be similar to the distribution of the DHPR α_2 subunit in dysgenic myotubes (Flucher et al., 1991). Finally, it is important to mention that the present

data cannot explain the low density of $I_{\beta\text{null}}$ and the absence of a significant amount of α_{1S} subunits in the transverse tubules previously inferred from charge movements (Strube et al., 1996). Recent studies indicate that DHPR β subunits play a role in targeting α_1 subunits to membrane sites (Chien et al., 1995). Expression of DHPR α_{1S} and β subunits in double-mutant $\text{mdg/mdg cchb1}^{-/-}$ myotubes may represent a useful system for exploring this dual role of DHPR β subunits in skeletal muscle.

Supported by the National Science Foundation and Centre National de la Recherche Scientifique U.S.-France Cooperative Research (INT-9603233 to CS and RC), the National Institutes of Health (HL-47053 to RC, PAP, and RGG), the National Science Foundation (IBN-93/9340 to RGG and PAP), the Muscular Dystrophy Association of America (JAP), and the Blakeslee Endowment Fund (JAP).

REFERENCES

- Adams, B. A., and K. G. Beam. 1989. A novel calcium current in dysgenic skeletal muscle. *J. Gen. Physiol.* 94:429–444.
- Adams, B. A., and K. G. Beam. 1991. Contraction of dysgenic skeletal muscle triggered by a potentiated, endogenous calcium current. *J. Gen. Physiol.* 97:687–696.
- Adams, B. A., T. Tanabe, A. Mikami, S. Numa, and K. G. Beam. 1990. Intramembrane charge movement restored in dysgenic skeletal muscle by injection of dihydropyridine receptor cDNAs. *Nature*. 346:569–572.
- Bean, B. P., M. C. Nowicky, and R. W. Tsien. 1984. Beta-Adrenergic modulation of calcium channels in frog ventricular heart cells. *Nature*. 307:371–375.
- Beurg, M., M. Sukhareva, C. Strube, P. A. Powers, R. Gregg, and R. Coronado. 1997. Recovery of Ca^{2+} current, charge movements, and Ca^{2+} transients in myotubes deficient in dihydropyridine receptor β_1 subunit transfected with β_1 cDNA. *Biophys. J.* 73:807–818.
- Bourinet, E., G. W. Zamponi, A. Stea, T. W. Soong, B. A. Lewis, L. P. Jones, D. T. Yue, and T. P. Snutch. 1996. The α_1E calcium channel exhibits permeation properties similar to low-voltage-activated calcium channels. *J. Neurosci.* 16:4983–4993.
- Bournaud, R., T. Shimahara, L. Garcia, and F. Rieger. 1989. Appearance of the slow Ca^{2+} conductance in myotubes from mutant mice with “muscular dysgenesis.” *Pflugers Arch. Eur. J. Physiol.* 414:410–415.
- Bulteau, L., M. Cogne, C. Cognard, and G. Raymond. 1977. Reversal of the relative expression of cardiac and skeletal α_1 subunit isoforms of the L-type calcium channel during in vitro myogenesis. *Pflugers Arch. Eur. J. Physiol.* 433:376–378.
- Castellano, A., X. Wei, L. Birnbaumer, and E. Perez-Reyes. 1993. Cloning and expression of a third calcium channel beta subunit. *J. Biol. Chem.* 268:3450–3455.
- Chaudhari, N. 1992. A single nucleotide deletion in the skeletal muscle-specific calcium channel transcript of muscular dysgenesis (mdg) mice. *J. Biol. Chem.* 267:25636–25639.
- Chaudhari, N., and K. G. Beam. 1993. mRNA for cardiac calcium channel is expressed during development of skeletal muscle. *Dev. Biol.* 155: 507–515.
- Chien, A. J., X. L. Zhao, R. E. Shirokov, T. S. Puri, C. F. Chang, D. Sun, E. Rios, and M. M. Hosey. 1995. Roles of a membrane-localized beta subunit in the formation and targeting of functional L-type Ca^{2+} channels. *J. Biol. Chem.* 270:30036–30044.
- Conti, F., L. J. De Felice, and E. Wanke. 1975. Potassium and sodium current noise in the membrane of the squid giant axon. *J. Physiol. (Lond.)*. 248:45–82.
- Dirksen, R. T., and K. G. Beam. 1995. Single calcium channel behavior in native skeletal muscle. *J. Gen. Physiol.* 105:227–247.
- Dirksen, R. T., J. Nakai, A. Gonzalez, and K. G. Beam. 1997. The S5–S6 linker of repeat I is a critical determinant of the L-type Ca^{2+} channel unitary conductance. *Biophys. J.* 72:A245.

- Flucher, B. E., J. L. Phillips, and J. A. Powell. 1991. Dihydropyridine receptor α subunits in normal and dysgenic muscle in vitro: expression of α -1 is required for proper targeting and distribution of α -2. *J. Cell Biol.* 115:1345–1356.
- Garcia-Martinez, J., and K. G. Beam. 1994. Measurement of calcium transients and slow calcium current in myotubes. *J. Gen. Physiol.* 103:107–123.
- Garcia-Martinez, J., T. Tanabe, and K. G. Beam. 1994. Relationship of calcium transients to calcium currents and charge movements in myotubes expressing skeletal and cardiac dihydropyridine receptors. *J. Gen. Physiol.* 103:125–147.
- Gregg, R. G., A. Messing, C. Strube, M. Beurg, R. Moss, M. Behan, M. Sukhareva, S. Haynes, J. A. Powell, R. Coronado, and P. A. Powers. 1996. Absence of the β subunit (cchb1) of the skeletal muscle dihydropyridine receptor alters expression of the α (1) subunit and eliminates excitation-contraction coupling. *Proc. Natl. Acad. Sci. USA.* 93:13961–13966.
- Heinemann, S. H., and F. Conti. 1992. Nonstationary analysis and application to patch clamp recordings. *Methods Enzymol.* 207:131–148.
- Hullin, R., D. Singer-Lahat, M. Freichel, M. Biel, N. Dascal, F. Hofmann, and V. Flockerzi. 1992. Calcium channel β subunit heterogeneity: functional expression of cloned cDNA from heart, aorta and brain. *EMBO J.* 11:885–890.
- Itagaki, K., W. J. Koch, I. Bodi, U. Klockner, D. F. Sligh, and A. Schwartz. 1992. Native-type DHP-sensitive calcium channel currents are produced by cloned aortic smooth muscle and cardiac α 1 subunits expressed in *Xenopus laevis* oocytes and are regulated by α 2 and β subunits. *FEBS Lett.* 297:221–225.
- Kamp, T. J., M. T. Perez-Garcia, and E. Marban. 1996. Enhancement of ionic current and charge movement by coexpression of calcium channel β 1A subunit with α 1C subunit in a human embryonic kidney cell line. *J. Physiol. (Lond.)* 492:89–96.
- Knudson, C. M., N. Chaudhari, A. H. Sharp, J. A. Powell, K. G. Beam, and K. P. Campbell. 1989. Specific absence of the α_1 subunit of the dihydropyridine receptor in mice with muscular dysgenesis. *J. Biol. Chem.* 264:1345–1348.
- Lory, P., G. Varadi, and A. Schwartz. 1992. The β subunit controls the gating and the dihydropyridine sensitivity of the skeletal muscle Ca²⁺ channel. *Biophys. J.* 63:1421–1424.
- Lory, P., G. Varadi, D. F. Sligh, M. Varadi, and A. Schwartz. 1993. Characterization of β subunit modulation of a rabbit cardiac L-type Ca²⁺ channel α 1 subunit as expressed in mouse L cells. *FEBS Lett.* 315:167–172.
- Neher, E., and C. F. Stevens. 1975. Conductance fluctuations and ionic pores in membranes. *Annu. Rev. Biophys. Bioeng.* 6:345–381.
- Nishimura, S., H. Takeshima, F. Hofmann, V. Flockerzi, and K. Imoto. 1993. Requirement of the calcium channel β subunit for functional conformation. *FEBS Lett.* 324:283–286.
- Noceti, F., P. Baldelli, X. Wei, N. Qin, L. Toro, L. Birnbaumer, and E. Stefani. 1996. Effective gating charges per channel in voltage-dependent K⁺ and Ca²⁺ channels. *J. Gen. Physiol.* 108:143–155.
- Ohlndieck, K., F. N. Briggs, K. F. Lee, A. W. Wechsler, and K. P. Campbell. 1991. Analysis of excitation-contraction coupling components in chronically stimulated canine skeletal muscle. *Eur. J. Biochem.* 202:739–747.
- Pereon, Y., J. Navarro, and P. T. Palade. 1997. Expression of the dihydropyridine receptor α -1 subunit isoforms in adult rat and mouse skeletal muscle. *Biophys. J.* 72:A149.
- Perez-Garcia, M. T., T. J. Kamp, and E. Marban. 1995. Functional properties of cardiac L-type calcium channels transiently expressed in HEK293 cells. Role of α 1 and β subunits. *J. Gen. Physiol.* 105:289–306.
- Perez-Reyes, E., A. Castellano, H. S. Kim, P. Bertrand, E. Bagstrom, A. E. Lacerda, X. Wei, and L. Birnbaumer. 1992. Cloning and expression of a cardiac/brain β subunit of the L-type calcium channel. *J. Biol. Chem.* 267:1792–1797.
- Shimahara, T., and R. Bornaud. 1991. Barium current in developing skeletal muscle cells of normal and mutant mice fetuses with “muscular dysgenesis.” *Cell Calcium.* 12:727–733.
- Sigworth, F. J. 1980. The variance of sodium current fluctuations at the node of Ranvier. *J. Physiol. (Lond.)* 307:97–129.
- Singer, D., M. Biel, I. Lotan, V. Flockerzi, F. Hofmann, and N. Dascal. 1991. The role of the subunits in the function of calcium channel. *Science.* 253:1553–1557.
- Strube, C., M. Beurg, P. A. Powers, R. G. Gregg, and R. Coronado. 1996. Reduced Ca²⁺ current, charge movement, and absence of Ca²⁺ transients in skeletal muscle deficient in dihydropyridine receptor β 1 subunit. *Biophys. J.* 71:2531–2543.
- Strube, C., M. Sukhareva, P. A. Powers, R. G. Gregg, and R. Coronado. 1997. The L-type Ca²⁺ current of β -1 null myotubes is not a dysgenic current. *Biophys. J.* 72:A147.
- Tanabe, T., B. A. Adams, S. Numa, and K. G. Beam. 1991. Repeat I of the dihydropyridine receptor is critical in determining calcium channel activation kinetics. *Nature.* 352:800–803.
- Tanabe, T., K. G. Beam, B. A. Adams, T. Niidome, and S. Numa. 1990a. Regions of skeletal muscle dihydropyridine receptor critical for excitation-contraction coupling. *Nature.* 346:567–569.
- Tanabe, T., K. G. Beam, J. A. Powell, and S. Numa. 1988. Restoration of excitation-contraction coupling and slow calcium current in dysgenic muscle by dihydropyridine receptor complementary DNA. *Nature.* 336:134–139.
- Tanabe, T., A. Mikami, S. Numa, and K. G. Beam. 1990b. Cardiac-type excitation-contraction coupling in dysgenic skeletal muscle injected with cardiac dihydropyridine receptor cDNA. *Nature.* 344:451–453.
- Tsien, R. W., B. P. Bean, P. Hess, J. B. Lansman, B. Nilius, and M. C. Nowicky. 1986. Mechanism of calcium channel modulation by β -adrenergic agents and dihydropyridine calcium agonists. *J. Mol. Cell. Cardiol.* 18:691–710.
- Varadi, G., P. Lory, D. Schultz, M. Varadi, and A. Schwartz. 1991. Acceleration of activation and inactivation by the β subunit of the skeletal muscle calcium channel. *Nature.* 352:159–162.
- Varadi, G., G. Mikala, P. Lory, M. Varadi, B. Drouet, M. Pincon-Raymond, and A. Schwartz. 1995. Endogenous cardiac Ca²⁺ channels do not overcome the E-C coupling defect in immortalized dysgenic muscle cells: evidence for a missing link. *FEBS Lett.* 386:405–410.
- Wei, X., E. Perez-Reyes, A. E. Lacerda, G. Schuster, M. A. Brown, and L. Birnbaumer. 1991. Heterologous regulation of the cardiac Ca²⁺ channel α 1 subunit by skeletal muscle β and γ subunits. *J. Biol. Chem.* 266:21943–21947.
- Yang, J., P. T. Ellinor, W. A. Sather, F. J. F. Zhang, and R. W. Tsien. 1993. Molecular determinants of Ca²⁺ channel selectivity and ion permeation in L-type Ca²⁺ channels. *Nature.* 366:158–161.